The First Broad-Range CO Ladders from the M83 and 30 Doradus

Ronin Wu[1]

[1]*Laboratoire AIM, CEA/DSM - CNRS - Irfu/Service d'Astrophysique, CEA Saclay, France*

ABSTRACT

We present the spectral observation results from M83 and 30 Doradus, using the Spectral and Photometric Imaging REceiver (SPIRE) of the *Herschel Space Observatory*. The warm CO lines covered in this wavelength include J =4–3 to J =13–12 transitions, which allow us to determine the peak CO ladder intensities and beyond. We model the physical conditions in the objects (N(CO), $T_{\rm kin}$, $n(H_2)$) using a large velocity gradient (LVG) code. We also investigate the [N II] 205 μm map from M83 and compare our result with the CO J =1–0 and Hα maps.

1. INTRODUCTION

M83 is a nearby starburst spiral galaxy at 5 Mpc away. Structure-wise, it is very similar to the Milky-way, and its face-on orientation makes it ideal to study the star-forming regions inside. 30 Doradus is a giant H II region in the Large Magellanic Cloud 50 kpc away from the Milky-Way. It is the brightest star-forming region in the LMC. We compare the CO lines observed by the *Herschel* SPIRE FTS from these two objects in this poster. The wavelength covered by the SPIRE FTS provides an unprecedented detection of the molecular features at the peak of the CO energy distribution.

2. DATA

We obtain the spectral data with both short-wavelength (SSW; 960 $< \nu <$ 1545 GHz) and long-wavelength (SLW; 450 $< \nu <$ 990 GHz) modules. The observation is part of the *Herschel* Guaranteed Time Key Programs, Very Nearby Galaxies Survey (VNGS, P.I. Chris Wilson) for M83 and Survey with *Herschel* of the ISM in Nearby Infrared Galaxies (SHINING, P.I. Eckhard Sturm) for 30 Doradus. We compare the CO spectral line energy distribution from the center of M83 ($13^h37^m0^s.9$, −29 deg 51′56.″78) and at ($5^h38^m49^s.61$, −69 deg 4′29.″64) from 30 Doradus. At these two chosen pointings, the central bolometers, SLWC3 and SSWD4, of the SLW and SSW modules are concentric. Before comparison, the two spectra are corrected for the objects' spatial light distribution, taking into account that the beam full-width-half-maximum (FWHM) varies from ∼ 20″ to ∼ 40″, using the method discussed in Wu et al. (2013). After correction, since the spatial distribution of the emission from both M83 and 30 Doradus is quite extended relative to the largest beam FWHM (41.″7) of the SPIRE FTS, the effective beam FWHM of the corrected spectrum can be approximated as 41.″7. The corrected spectrum of M83 is presented in Figure 1.

The M83 is observed in the full-sampling mode. The complete Nyquist sampled map of the SPIRE FTS has a bolometer spacing of ∼12.″7. We also compare the [N II] 205 μm map of M83 with star-formation rate (SFR), calculated with the far-UV (FUV) and the 24 μm maps of M83 using the calibration given in Hao et al. (2011). The details of the map-making procedure is described in Wu et al. (2014, in preparation).

3. RESULTS

3.1. Comparison of the Star-forming Regions in M83 and 30 Doradus

Figure 2 compares the SLEDs from M83 and 30 Doradus from the pointings described in the previous section where the two central bolometers of SLW and SSW are concentric. Based on the SPIRE FTS observation, the distribution of the CO lines from M83 nucleus follows a similar trend as the observed result from M82 (Kamenetzky et al. 2012). However, the CO lines from 30 Doradus imply a rather high kinetic temperature with prominently excited high-J, e.g. J =12–11, CO lines and its SLED peaking beyond the bandwidth of the SPIRE FTS. We analyze the temperature compositions from the two SLEDs with a radiative transfer model which assumes local statistical equilibrium (RADEX; van der Tak et al. 2007). The interpretation from the model indicates that the fraction of warm-to-cold CO component is approximately 0.01 from the observed region in M83 and is nearly 1 from the observed region in 30 Doradus. At the distance to M83, the observed region is approximately 1 kpc. For 30 Doradus, the observed region is approximately 10 pc. The difference observed in Figure 2 can possibly be explained by the relative distance to the observed star-forming region. This result clearly reveals the interaction of the molecular cloud and star-formation and can help determine the cooling efficiency contributed by CO molecules in photo-dissociation regions (PDRs).

3.2. Using [N II] to Trace Star Formation?

To investigate how the [N II] 205 μm and $\Sigma_{\rm SFR}$ relate to each other and how this relationship compares with the existing one between $\Sigma_{\rm SFR}$ and CO J =1–0 transition from M51 (Kennicutt et al. 2007), we compare the pixel-by-pixel values of

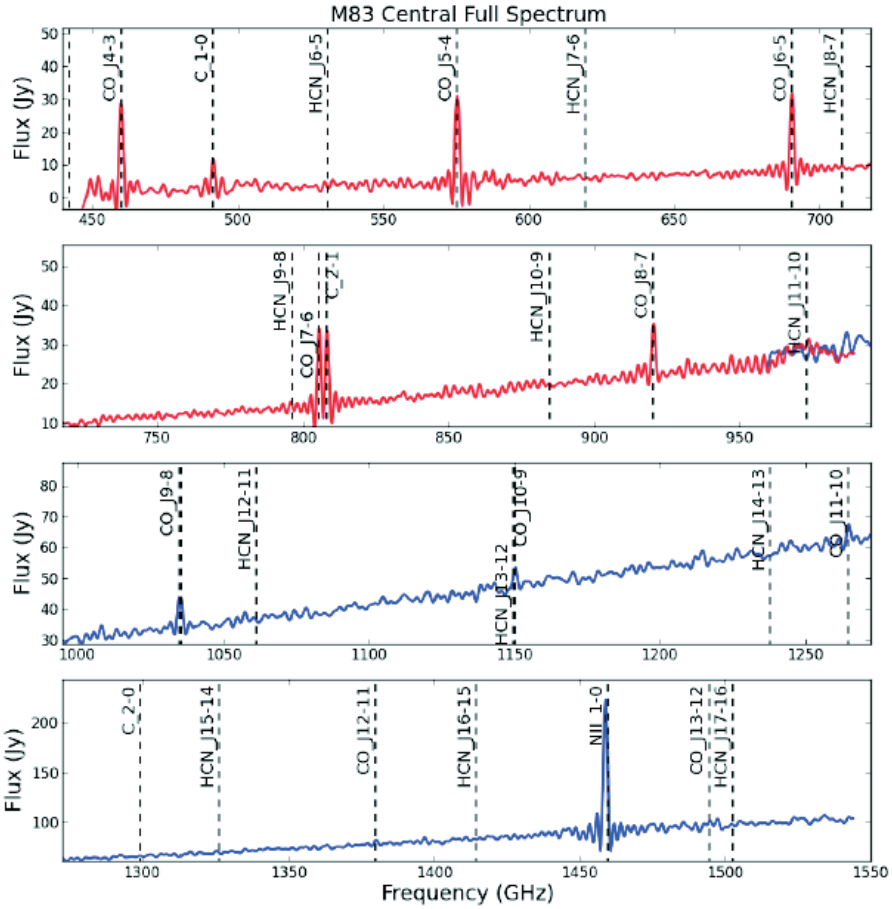

Figure 1. The spatial light distribution corrected spectrum from the M83 nucleus.

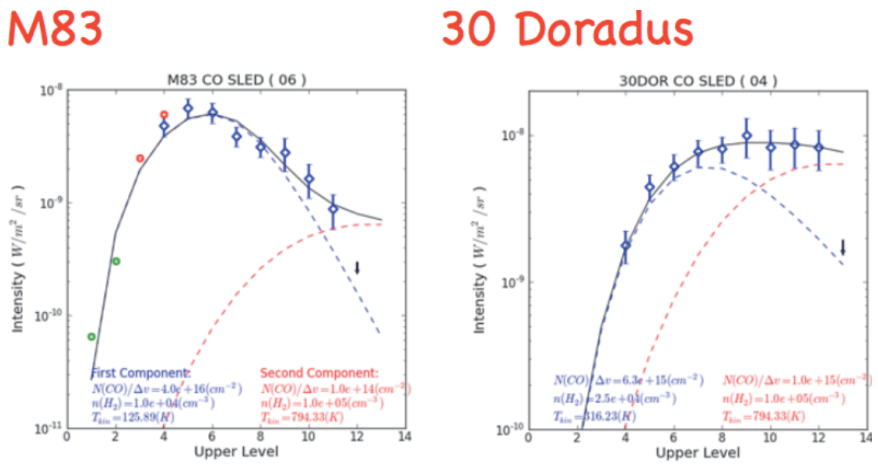

Figure 2. A comparison of the CO SLEDs from M83 and 30 Doradus.

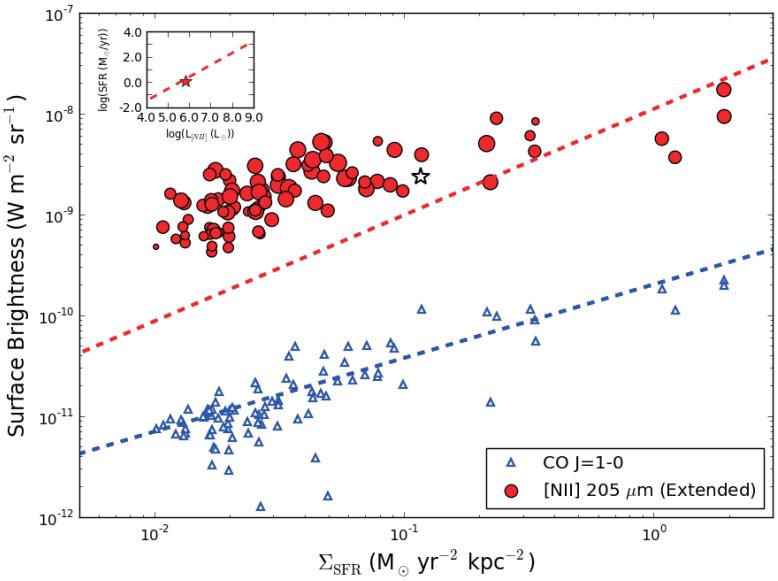

Figure 3. Comparison of the [N II] 205 μm, $S_{CO(1-0)}$, and, Σ_{SFR}. The embedded figure shows the integrated properties of M83 on the relationship calibrated with a sample of ULIRGs and star-forming galaxies (Wu et al. 2014, in preparation).

the [N II] 205 μm surface brightness with the Σ_{SFR}, and of the $S_{CO(1-0)}$ with Σ_{SFR}, which is calculated from the FUV and 24 μm photometry maps of M83 following the calibration given in Hao et al. (2011). Figure 3 shows that the values of [N II] 205 μm follow a close relationship with the Σ_{SFR}, and when compared with the $S_{CO(1-0)}$, the surface brightness of [N II] 205 μm is generally around two orders of magnitudes higher. A recent work by Zhao et al. (2013) has shown that the [N II] 205 μm luminosity holds the following relationship with the total SFR (calibrated with the total infrared luminosity, L_{IR}), among a sample of 70 luminous infrared galaxies (LIRGs) and 30 star-forming galaxies. Figure 3 also compares the $S_{CO(1-0)}$ with Σ_{SFR}. The calibration of Σ_{SFR}, estimated by the Hα surface brightness, as a function of Σ_{H_2}, estimated by the CO J =1–0 intensity (I_{CO}; Kennicutt et al. 2007), is indicated by the blue dashed line.

4. CONCLUSION

We show the *Herschel* SPIRE FTS observations from the regions inside the M83 spiral arms and 30 Doradus. We successfully corrected the spectra from the concentric central bolometers of SPIRE FTS by taking into account the source distribution-beam coupling effect. Comparison of the M83 nucleus and 30 Doradus CO SLED shows that a higher portion of warm molecular gas is present in 30 Doradus. A good correlation is found between the [N II] 205 μm and SFR surface density. However, we observe a disagreement from the fainter [N II] 205 μm regions with the trend demonstrated by bright [N II] 205 μm regions. Caution should be exercised before one applies this line as a general SFR tracer.

REFERENCES

Hao, C.-N., Kennicutt, R. C., Johnson, B. D., et al. 2011, ApJ, 741, 124
Kamenetzky, J. R., Glenn, J., Rangwala, N., et al. 2012, ApJ, 753, 70
Kennicutt, R. C., Calzetti, D., Walter, F., et al. 2007, ApJ, 671, 333
van der Tak, F. F. S., Black, J. H., Schöier, F. L., et al. 2007, A&A, 468, 627
Wu, R., Polehampton, E. T., Etxaluze, M., et al. 2013, A&A, 556, A116
Zhao, Y., Lu, N., Xu, C. K., et al. 2013, ApJ, 765, L13